Reliability and cost–benefits of adding alternate power sources to an independent micro-grid community

M. Tanrioven *

Department of Electrical Engineering, Yildiz Technical University, Besiktas, Istanbul, 34349, Turkey

Abstract

Interest in alternative energy resources such as wind, solar energy and fuel cell (FC) has been on the increase due to improved public awareness of the high energy cost and adverse environmental impacts of conventional energy sources. Therefore, the rapid growth and potential future demand for these energy sources suggest a need to consider both reliability and cost–benefits of the supply for each case. This paper presents a simulation methodology for reliability and cost assessment of these energy sources in an independent micro-grid (IMG) system, which is a distribution system with distributed energy sources such as micro-turbine, photovoltaic and fuel cells. A systematic technique and a computer program for reliability and cost assessment of the IMG system containing FC, photovoltaic (PV) and wind energy (WE) have been developed. The adequacy of the IMG is evaluated in three steps: (i) atmospheric data is generated for PV and WE in addition to the development of a 50 kW PEM FC generation and energy conversion model, (ii) the power delivered by these energy sources is calculated, and (iii) system adequacy and energy indices are calculated based on the system load balance equation, which is the combination of generated power and system load demand. The suggested technique can then be used to help system planners to provide objective indicators for suitable installation locations, operating policies, and energy type and size selection for IMG system containing alternative energy sources.
© 2005 Elsevier B.V. All rights reserved.

Keywords: PEM fuel cell; Photovoltaic; Wind turbine; Renewable energy; Reliability; Economic evaluation

1. Introduction

The concept of the micro-grid was introduced as a radial or networked distribution system with distributed energy sources such as a fuel cell (FC), photovoltaic (PV) and wind energy (WE power sources). The application of these alternative energy sources in the new competitive electric power marketing has gained significant attention in recent years due to economic and environmental concerns over fossil and nuclear fuel based electrical energy, as well as reduction of fossil resources. Although they are known as environmentally friendly, not all the alternative sources of energy are an reliable, cost effective and efficient as desired. However, it is possible to design an efficient, reliable and cost effective independent micro-grid (IMG) system by utilizing various combinations of the alternative sources of energy. In this re-

spect, it is vital to assess the reliability level and economic benefits of utilizing FC, PV and WE as well as diesel generators (DG) in different configurations. Some of the key factors that affect the reliability of the IMG system are the limitations in the available energy from alternative sources and their varying behavior. Hence, it is quite evident that the reliability of the supply and the corresponding cost–benefits should be evaluated together.

The reliability aspects of alternative sources of energy are of growing importance. This is largely because of the fact that renewable energy sources are contributing to major power systems more than in the past. As a consequence a relatively high penetration of these sources in the IMG system can make a considerable impact on the reliability and cost.

Although FC power plants have a fixed output, the total IMG system has a fluctuating output because of the varying characteristics of the PV and WE. For this reason, the behavior of the IMG system with renewable sources should be characterized by the random variables of which the number

* Tel.: +90 212 2597070.
E-mail address: tanriov@yildiz.edu.tr.

increases in proportion to the number of renewable sources in the system. Accordingly, probabilistic approaches must be used for a realistic reliability and cost assessment. However, not all the system behaviors can be explained by probabilistic techniques, but also there are system behaviors for determination of system capacity requirements such as loss of more than one small unit or loss of the largest/large unit, which can be evaluated by better deterministic methods [1]. As a consequence, an evaluation methodology is needed in order to combine probabilistic and deterministic methods in a unique approach, i.e. system well-being approach that incorporates deterministic criteria into stochastic behavior [2,3].

This paper uses a well-being approach in order to make an evaluation of system reliability/cost indices. The evaluation of these indices are illustrated by specifying reliability/adequacy and cost indices for different alternative sources of energy additions.

2. Adequacy assessment of IMG system

The performance of the system can be monitored using well-being analysis that combines deterministic considerations and probabilistic indices. The adequacy of the IMG system herein considered to be situated in one of the operating states designated as healthy, marginal and risky as shown in Fig. 1. In the healthy state, all the operating constraints and components such as line, transformers and breakers are within the minimum and maximum limits, demonstrating that the system has the capacity to supply the load without overloading any equipment. In this state, there is sufficient equipment such that loss of any components specified by deterministic criteria, e.g. outage of a transformer will not result in load curtailment. In the marginal state, the system still has the ability to provide the system requirements, but there is no longer sufficient margin to meet the specified deterministic criteria. In the risky state, the generating system has an inability to satisfy the load requirements.

Each system state is characterized in terms of available margin that is the difference between the existing power capacity and the load. Conceptual tasks associated with each system state characterization and adequacy assessment of IMG system is illustrated as in Fig. 2.

Firstly, an outage history of each individual generating unit is created on a time dependent basis as illustrated in Fig. 3. Afterward, a state history of the generation capacity of entire system is obtained by combining the outage records of all the units in the IMG system.

The probabilities of system states, $P(h)$, $P(m)$ and $P(r)$ can be easily calculated using the contingency enumeration method (CEM), which utilizes a generation model for dif-
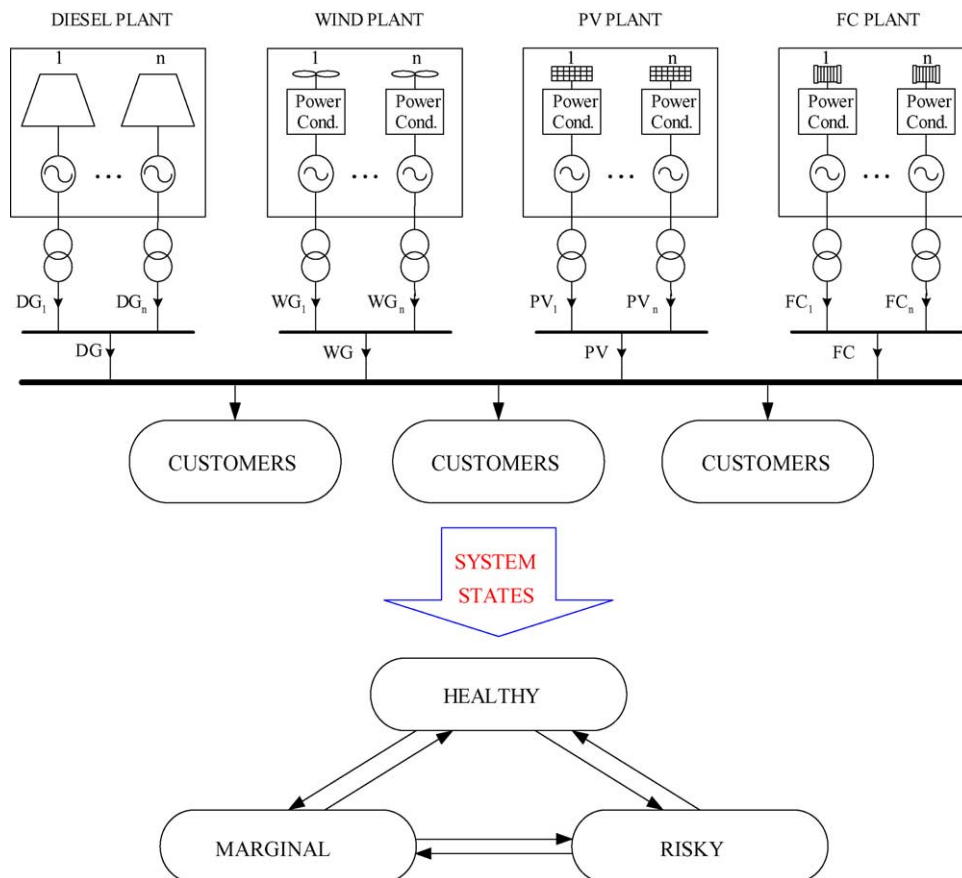

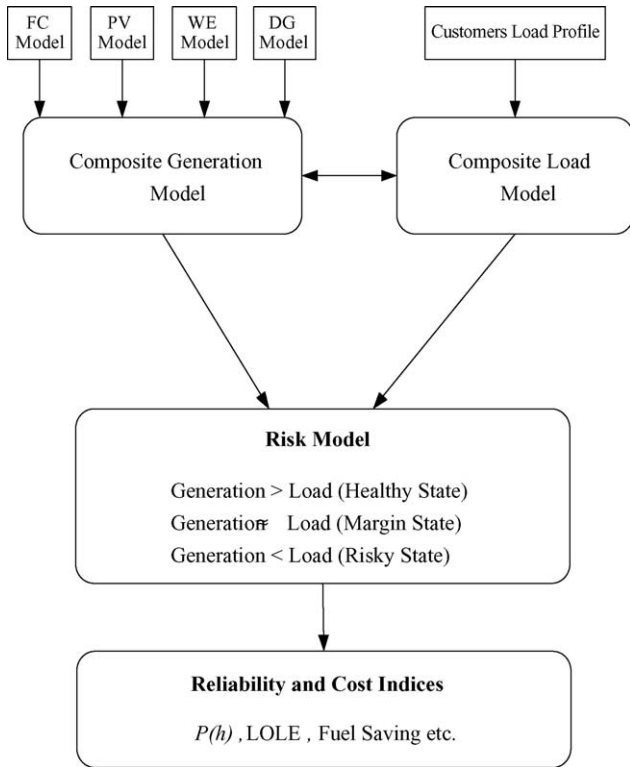Fig. 1. Typical IMG system and its well-being model.

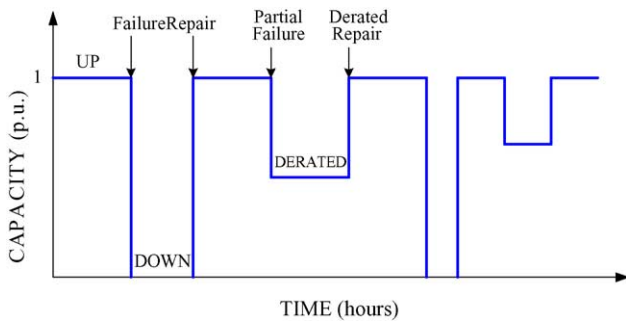Fig. 2. Conceptual tasks for generating capacity evaluation of IMG system.

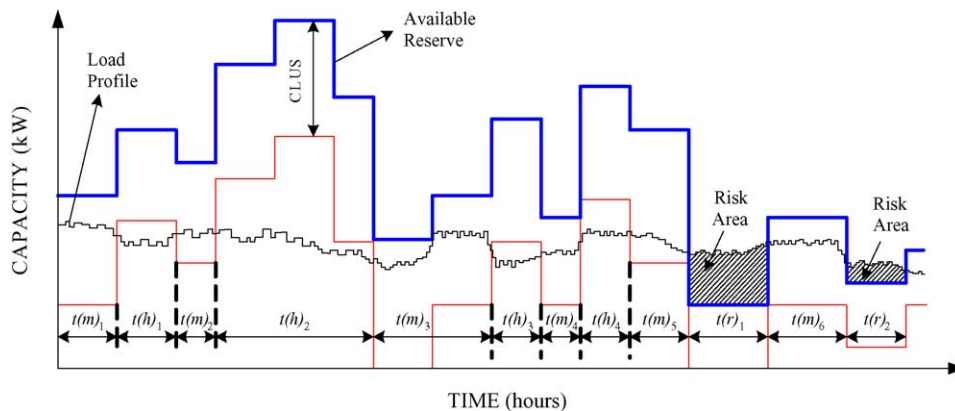Fig. 3. State history of a generating unit vs. time.

ferent potential combinations of the existing generating unit outages, their probabilities and capacity of the largest unit associated with each contingency state (CLUS) [4]. As shown in Fig. 4, each contingency in the generation model is compared with the corresponding system load to determine the amount of capacity reserve available at each condition. When the system load profile is less than or equal to available reserve, that particular contingency is considered to be healthy and its duration is measured as $t(h)_i$. On the other hand, when the load profile is less than or equal to total capacity profile but greater than the CLUS profile, then the contingency state is said to be marginal and its duration is given as $t(m)_i$. When the load profile is greater than the available capacity profile, the system state is called as risky with a duration of $t(r)_i$.

Monte Carlo simulation (MCS) method can be used to estimate the indices that represent system states and behavior by simulating the actual process and random behavior of the system. For the IMG system, the hourly power output from PV and WE is combined with the outputs of FC unit and the existing DG units in the system. The outage history of each energy unit can be generated by simulating its failure and repair versus time using Eqs. (1) and (2), respectively [5]:

$$T_{\text{on}} = -\text{MTTF} \ln(U) \tag{1}$$

$$T_{\text{off}} = -\text{MTTR} \ln(U') \tag{2}$$

where U and U' are the random numbers between 0 and 1, and MTTF (mean time to failure) and MTTR (mean time to repair) are the unit mean times to failure and repair, respectively.

Here, the probabilities associated with healthy, marginal and risky states are considered as operating criteria where probabilistic and deterministic criteria, i.e. healthy state definition are involved. In general, the probability of being in one of the three states can be expressed for 1-year basis as $P_i = $ (annual availability)/8760. If the available recorded data are given for periods of more than 1-year, then the probabilities associated with each of the state can be given as follows. Assume that $P(h)$, $P(m)$ and $P(r)$ are the probabilities of healthy, marginal and risky states, respectively, and can be evaluated using Eqs. (3)–(6), where N is the total num-

Fig. 4. Combining both generation and load profiles.

ber of simulated years, $n(h)$, $n(m)$ and $n(r)$ are the number of healthy, marginal and risky states, respectively, and their durations are $t(h)$, $t(m)$ and $t(r)$ [6]:

$$P(h) = \frac{\sum_{i=1}^{n(h)} t(h)_i}{N \times 8760} \tag{3}$$

$$P(m) = \frac{\sum_{i=1}^{n(m)} t(m)_i}{N \times 8760} \tag{4}$$

$$P(r) = \frac{\sum_{i=1}^{n(r)} t(r)_i}{N \times 8760} \tag{5}$$

$$P(h) + P(m) + P(r) = 1 \tag{6}$$

The model applicable for reliability and cost evaluation of IMG system including energy sources of FC, PV and WE is presented in the following section.

3. Development of overall system evaluation model

The adequacy assessment of IMG system having FC, PV and WE has been evaluated using chronological simulation. The fundamental process can be expressed in brief as follows:

1. The models of alternative energy sources in the IMG system are developed.
2. Atmospheric data for PV and WE is generated.
3. The power from PV and WE is combined with the outputs of FC unit and the existing DG units in the system.
4. The generated power profile from step 3 is combined with system load profile.
5. Form and calculate the required reliability and cost indices by observing the system capacity reserve model obtained in the fourth step.

The evaluation model is illustrated as shown in Fig. 5. The main difficulty positioned in the model is the reliability evaluation of FC system. This is mostly originated from the
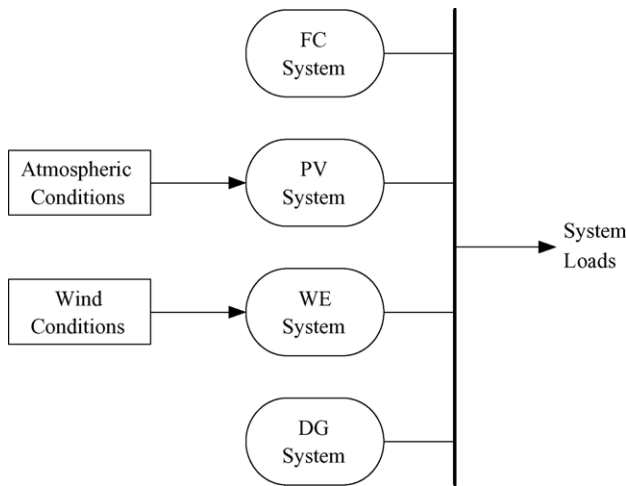

Fig. 5. The adequacy evaluation model for IMG system containing FC, PV, WE and DG systems.

fact that the application of FC systems is recently emerging technology with insufficient data and a number of uncertainties, and so the FC reliability indices such as MTTF, MMTR and FOR (forced outage rate) should be estimated in order to perform overall system reliability evaluation. Therefore, a new systematic technique for PEM (proton exchange membrane) FC system reliability assessment has been developed. It includes development of a state-space generation model for PEM fuel cell and calculates the system availability and reliability indices.

3.1. Modeling FC system

Fuel cells basically convert chemical energy of hydrocarbon fuels, typically hydrogen directly into dc form of electrical energy. A FC based power system mainly consists of a fuel-processing unit (reformer), FC stack and power conditioning unit. The FC uses hydrogen as input fuel and produces dc power at the output of the stack. A simple representation of FC system is given in Fig. 6.

The performance of a FC is generally characterized by using the polarization curve, which is a plot of the FC voltage versus load current. The polarization curve is computed by using the Tafel equation [7], which subtracts the various voltage losses from the open circuit dc voltage, and is expressed as

$$V_{\text{stack}} = V_{\text{open}} - V_{\text{ohmic}} - V_{\text{activation}} - V_{\text{concentration}} \tag{7}$$

where

$$V_{\text{open}} = N_0(E^0 + E^1)$$
$$= N_0 \left[-\frac{\Delta \bar{g}_f^0}{2F} + \frac{RT}{2F} \ln \left(\frac{p_{\text{H}_2} \sqrt{p_{\text{O}_2}}}{p_{\text{H}_2\text{O}}} \right) \right] \tag{8}$$

$$V_{\text{ohmic}} = (i + i_n)R_{\text{FC}} = I_{\text{dc}} R_{\text{FC}} \tag{9}$$

$$V_{\text{activation}} = N_0 \frac{RT}{2\alpha F} \ln \left(\frac{I_{\text{dc}}}{I_0} \right) \tag{10}$$

$$V_{\text{concentration}} = -c \ln \left(1 - \frac{I_{\text{dc}}}{I_{\text{Lim}}} \right) \tag{11}$$

In the above equations, N_0 is the cell number, V_0 the open cell voltage, R the universal gas constant, T the temperature of the fuel cell stack, F the Faraday's constant, P_{H_2} the hydrogen partial pressure, $P_{\text{H}_2\text{O}}$ the water partial pressure, P_{O_2} the oxygen partial pressure, P_0 the standard pressure, α the charge transfer coefficient of the electrodes, I_{dc} the current of the FC stack, I_{Lim} the limiting current of FC stack, I_0 the exchange current of FC stack and c the empirical coefficient for concentration voltage. The steady state voltage and power for one cell ($N_0 = 1$) versus cell current density is obtained based on Eq. (7) as shown in Fig. 7. In the figure, the current density, i, is defined as current per active area $i = I_{\text{dc}}/A_{\text{act}}$. Due to series connection of cells in a stack, the total stack voltage is calculated as $V_{\text{dc}} = N_0 V_{\text{cell}}$ and the stack power is defined as $P = V_{\text{dc}} I_{\text{dc}}$.
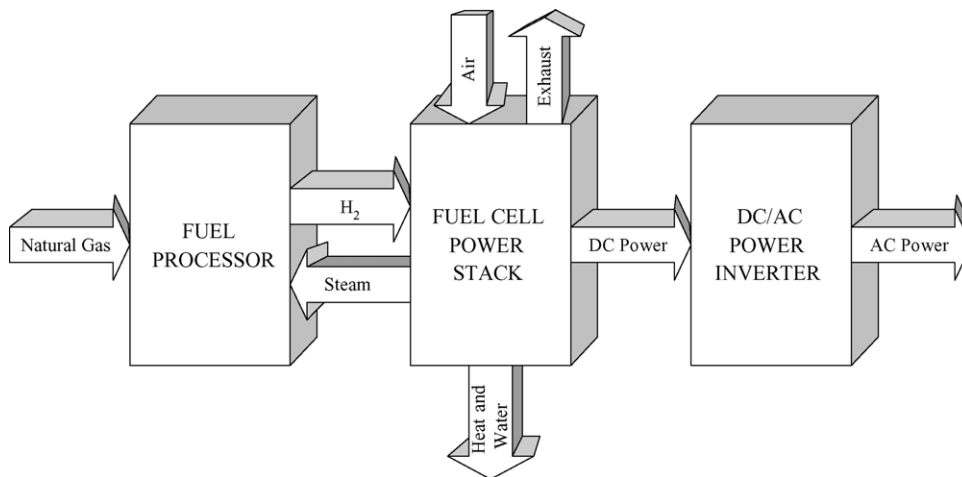
Fig. 6. Basic fuel cell components.

Although the basic concept of working of a fuel cell is quite simple, there are many auxiliary devices working behind the scene in order to operate the FC smoothly and efficiently. These devices that take part in the gas and electricity management are used in order for regulating the parameters such as reactant flow rate, total pressure, reactant partial pressure, temperature, and membrane humidity at a desired value. Hence, FC can run smoothly without getting the stack either flooded or drying out [8]. Accordingly, any malfunctioning, performance loss and/or failure in these auxiliaries can lower the overall performance of the fuel cell. Various auxiliary components such as air compressors, pumps, humidification equipment, blower and coolers are used in the FC system that are all related to thermodynamics and flow control. Besides, the components such as power conditioning unit (dc/dc converter plus dc/ac inverter), control electronics, energy storage and transformer take part in power conversion and overall system control. Fig. 8 shows a PEM fuel cell system block diagram that shows the auxiliary components along with input and output signals.
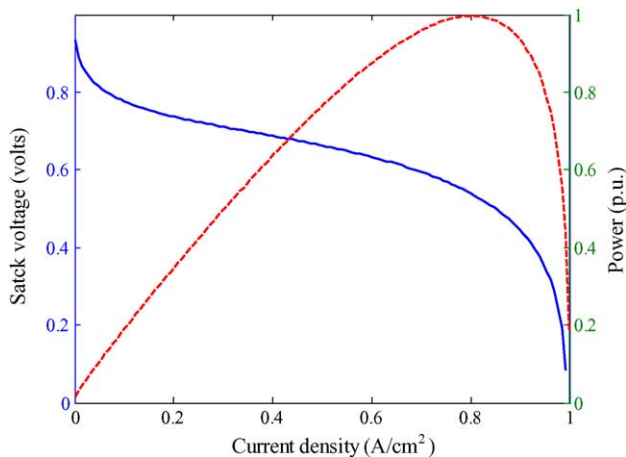
Since FC generation units requires a number of auxiliary equipment for smooth and efficient operation, they are subject to different possible derated capacity states based on the factors such as partial or full failure of auxiliaries and deterioration of fuel quality [8–10]. During normal operation, the fuel cell system components such as compressor, fans, pumps, motors, temperature and humidity sensors, relays, and other control electronics could contribute to a system failure or derated mode by different reasons such as ignition of any leaking hydrogen, material fatigues, wear outs, break downs, membrane drying out, overheating, and freezing of water in channels, etc. [8]. If any of the components go beyond its operating limits for some reasons, the output of the FC power plant will be reduced by a factor. For instance, insufficient circulating coolant flow due to the failure of coolant water pump may cause the nominal output to be reduced. Certain other failures may cause either a reduction in nominal output power or total system outage.

Tanrioven et al. [11] developed a FC reliability assessment model based on the possible results of aforementioned auxiliary failures to calculate the effects of performance reduction in FC sub-systems on overall FC performances. The model developed in Ref. [11] can be summarized as in Fig. 9, where λ is the failure rate and μ the repair rate.

The authors simulates the operating cycles associated with up, derated and down states on the conditions that there are partial/full failures or insufficiencies with respect to cooling, humidification, fueling, air supply and energy storage systems. Derated level of FC output power is expressed in terms of percent reduction in power supplying capacity of FC. Table 1 summarizes the effects of inadequacies/failures of FC sub-systems on the system output power with their state-space models.

The state-space based reliability calculation is performed using Markov models. The system equation of Fig. 9 can be written in the form of state-space as $dP(t)/dt = AP(t)$, where $P(t)$ is the probability vector of all states and A the transition

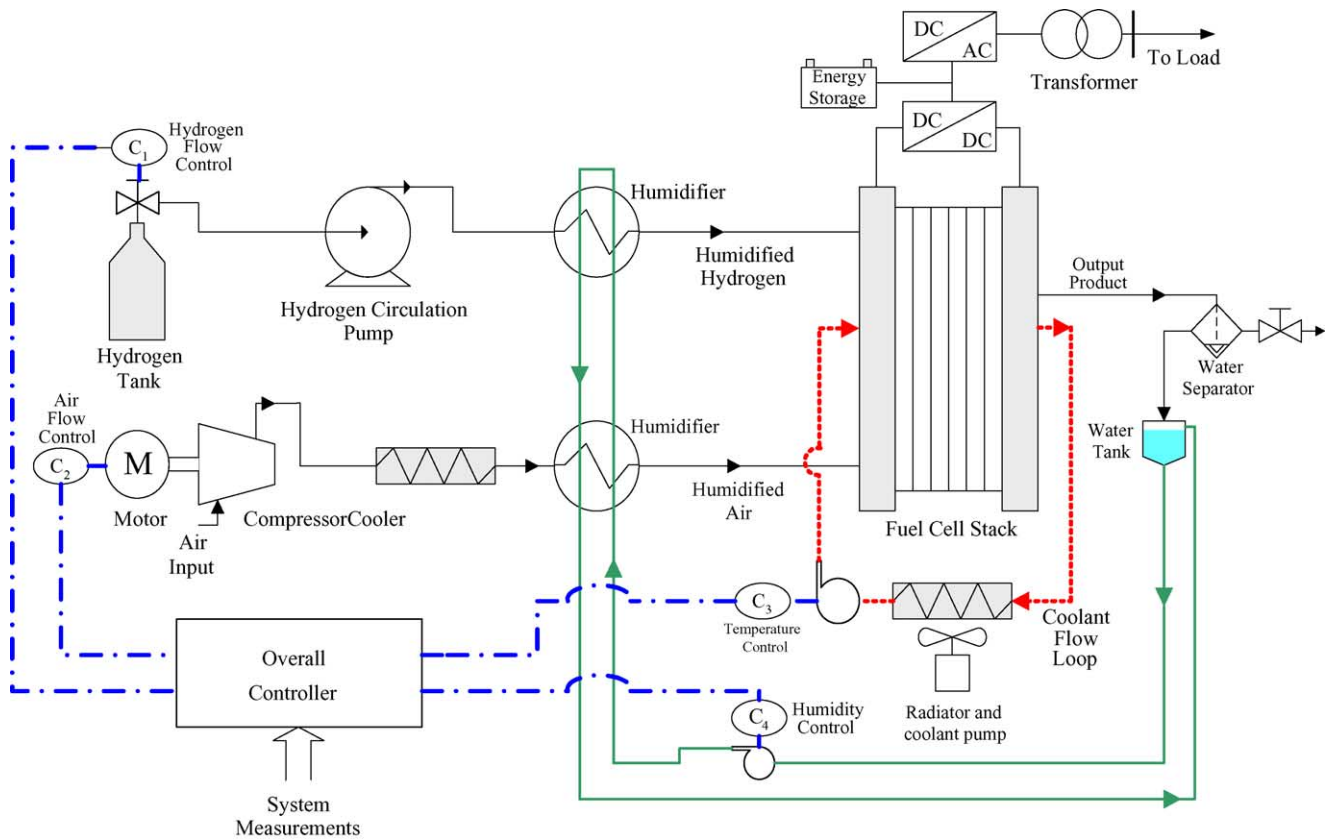Fig. 7. One-cell voltage and power vs. current density.

Fig. 8. PEM fuel cell system block diagram.

matrix. State transitions in Markov processes occur continuously rather than at discrete time intervals and both system states and transition rates together constitute state-space diagram, and herein failure and repair rates are equivalent to
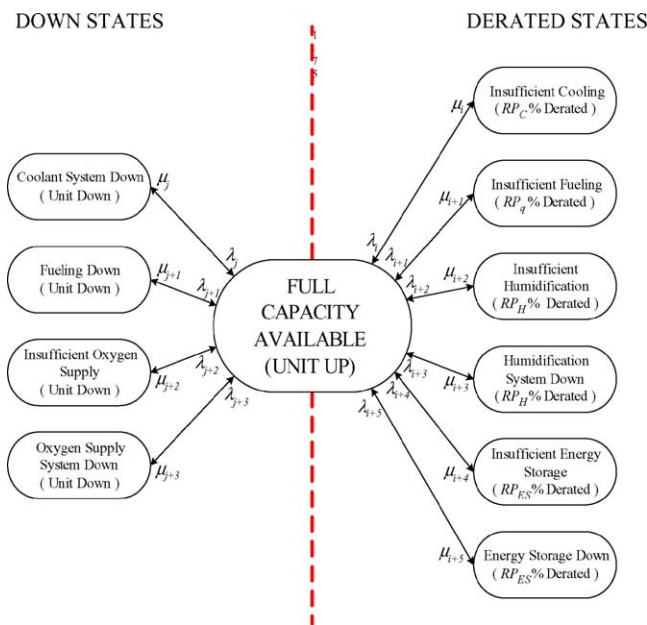

Fig. 9. The state-space model of the FC generating unit.

state transition rates, which are estimated in [11] by Weibull distribution model.

Since FC technology is so young and there is no publicly available data associated with the failures of FC system, a fuzzy logic rule-base system is formed based on the expert knowledge, derived from conventional system failure, to determine the performance loss of system auxiliary. In this standpoint, the rule format for non-healthy state level is given as below.

If input is ⟨component age and maintenance cycle and . . .⟩ then, output is ⟨degree of failure severity⟩.

As a result, any of the reliability indices associated with FC availability can be obtained using the model reported in Ref. [11]. For instance, total duration of up and down phases can be calculated, respectively, as $t_{up} = A \times 8760$ and $t_{down} = (1 - A) \times 8760$ as well as the total duration of derated system state of FC system can be obtained in hours as $t_i = (1 - A_i) \times 8760$, where A_i is the availability of derated FC states that result in lack of supply.

3.2. Modeling PV system

Solar cell is the basic unit of the photovoltaic generator, which converts the Sun's rays or photons directly to electrical energy. A solar cell is generally represented by circuit

Table 1
Summary of state-space model of FC system associated with each of system auxiliaries
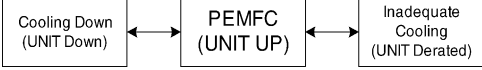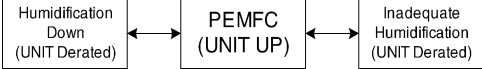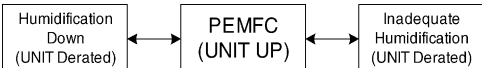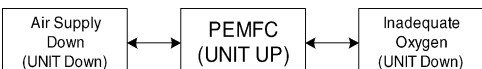
FC sub-systems	Failure severity	FC system	State-space representation			Possible inadequacy effects on system output
Cooling system	Inadequacy	Derated	Cooling Down (UNIT Down)	PEMFC (UNIT UP)	Inadequate Cooling (UNIT Derated)	Output power will be derated by RP_c (%) due to increase in temperature and internal resistance
	Down	Down				
Humidification system	Inadequacy	Derated	Humidification Down (UNIT Derated)	PEMFC (UNIT UP)	Inadequate Humidification (UNIT Derated)	Output power will be derated by RP_H (%) due to increase in internal resistance and decrease in partial pressure of the reactants
	Down	Derated				
Fueling system	Inadequacy	Derated	Humidification Down (UNIT Derated)	PEMFC (UNIT UP)	Inadequate Humidification (UNIT Derated)	Output power will be derated by RP_q (%) due to decrease in hydrogen supply and/or degeneration of pure hydrogen
	Down	Down				
Air supply system	Inadequacy	Down	Air Supply Down (UNIT Down)	PEMFC (UNIT UP)	Inadequate Oxygen (UNIT Down)	Relative inadequacy of air supply will not lead reduction in output power, but may result in complete system failure if it is so severe
	Down	Down				
Energy storage system	Inadequacy	Derated	Energy Storage Down (UNIT Derated)	PEMFC (UNIT UP)	Inadequate Energy Storage (UNIT Derated)	Output power will be derated by RP_{ES} (%) due to FC stack and battery degradation
	Down	Derated				

diagram as shown in Fig. 10. Photo-current source, I_{ph}, one diode, and a series resistance, R_s that represents the internal resistance of each cell plus connection resistance between cells are included, but the shunt resistance is excluded in the model.

The PV system model can be developed based on current (I)–voltage (V) characteristic of the modules. The I–V characteristic of the solar cell is given based on the diode model as follows [12]:

$$I = I_{ph} - I_D = I_{ph} - I_0[e^{q(V+IR_S)/AkT} - 1] \tag{12}$$

where A is the diode quality factor, k the Boltzmann's gas constant, T the absolute temperature of the cell, q electronic charge and V the voltage induced across the cell. I_0 is the dark saturation current and depends on temperature. The power delivered from a PV cell can be estimated from its I–V curves, as shown in Fig. 11, the data for which is available from the manufacturer.

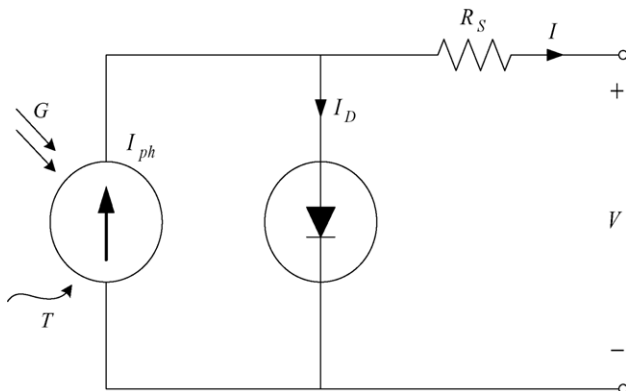Eq. (12) is implicit and nonlinear, and thus performing an analytical solution is complicated. The parameters in the model vary with respect to irradiance (G), and temperature. The output current increases with an increase in solar radiation and the voltage level increases with a decrease in temperature.

The cells are connected in series to form a module and the modules are connected in parallel to form an array. The I–V curve for a PV module can be constructed by adding the I–V curves of the individual cells contained in it. Fig. 12 shows how the characteristic of I–V curve is modified in the cases of series and parallel connections, P_r.

A PV module consisting of n_p parallel branches, each with n_s solar cells in series is illustrated as shown in Fig. 13.

The model of PV module can be obtained by replacing each cell in Fig. 13 with the equivalent diagram of Fig. 10. The current of PV module, $I^{(m)}$ can be given under varying operating conditions as below:

$$I^{(m)} = I_{sc}^{(m)}[1 - e^{(V^{(m)} - V_{oc}^{(m)} + R_s^{(m)}I^{(m)})/n_s V_t^{(c)}}] \tag{13}$$

Fig. 10. The circuit diagram of the PV model.

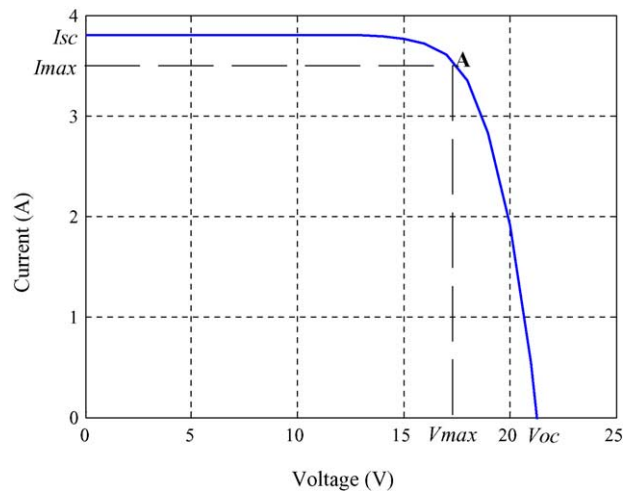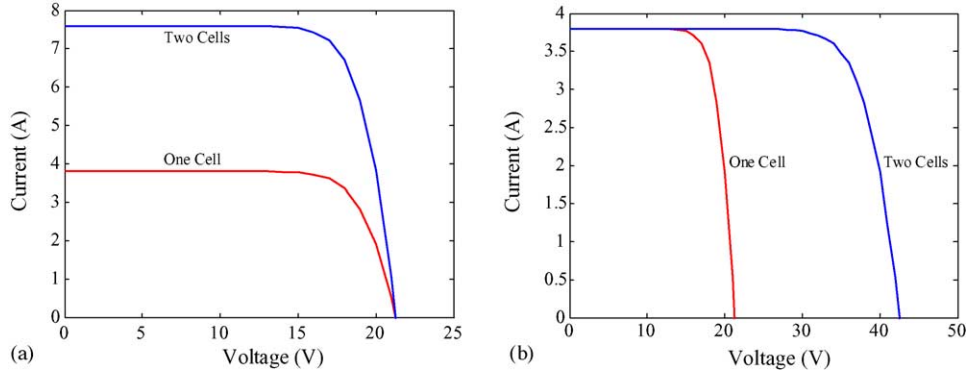
Fig. 11. *I*–*V* curve of a PV cell.

Fig. 12. Parallel (a) and (b) series connection of identical solar cells.

The expression for current of PV module, $I^{(m)}$ is implicit and nonlinear, and therefore determination of analytical solution is difficult. This is because of the fact that the module characteristics supplied by the manufacturer are usually determined under special conditions, e.g. standard conditions (irradiation is $1000\,W\,m^{-2}$, and cell temperature is $25\,°C$). Hence, the computation of the current should continuously be modified with respect to irradiance and temperature variation. The computation process used in PV module simulation consists of the following steps [13]:

- *Step 1*. The manufacturer's catalogues provides parameters, i.e. maximum power ($P_{max,0}^{(m)}$), short-circuit current ($I_{sc,0}^{(m)}$), open circuit voltage ($V_{oc,0}^{(m)}$), number of cells in series (n_s) and number of cells in parallel (n_p) associated with the PV module for standard conditions. Therefore, in the first step these data should be converted to cell level using the following equations, where the indices "0" and "(c)" indicate standard conditions and cell level parameters, respectively, and V_t the thermal voltage. In the equations, fill factor (FF) is the ratio of maximum power to product of

I_{sc} and V_{oc}:

$$P_{max,0}^{(c)} = \frac{P_{max,0}^{(m)}}{n_s n_p} \tag{14}$$

$$V_{oc,0}^{(c)} = \frac{V_{oc}^{(m)}}{n_s} \tag{15}$$

$$I_{sc,0}^{(c)} = \frac{I_{sc,0}^{(m)}}{n_p} \tag{16}$$

$$V_{t,0}^{(c)} = \frac{AkT_0}{q} \tag{17}$$

$$v_{oc,0} = \frac{V_{oc,0}^{(c)}}{V_{t,0}^{(c)}} \tag{18}$$

$$FF = \frac{v_{oc,0} - \ln(v_{oc,0} + 0.72)}{v_{oc,0} + 1} \tag{19}$$

$$FF_0 = \frac{P_{max,0}^{(c)}}{V_{oc,0}^{(c)} I_{sc,0}^{(c)}} \tag{20}$$

$$r_s = \frac{FF_0 - FF}{FF_0} \tag{21}$$

$$R_s^{(c)} = r_s \frac{V_{oc,0}^{(c)}}{I_{sc,0}^{(c)}} \tag{22}$$

- *Step 2*. Once the cell data are obtained from step 1, the next step is to determine the cell's parameter under operating conditions (T_a, G_a) using Eqs. (23)–(28), where the indices "nom" and "a" indicate nominal ($G_{nom} = 800\,W\,m^{-2}$ and $T_{a,nom} = 20\,°C$) and ambient conditions, respectively. If nominal cell temperature $T_{nom}^{(c)}$ is not provided by manufacturer, it is practical to estimate K_2 as $0.03\,cm^2\,W^{-1}$:

$$K_1 = \frac{I_{sc,0}^{(c)}}{G_0} \tag{23}$$

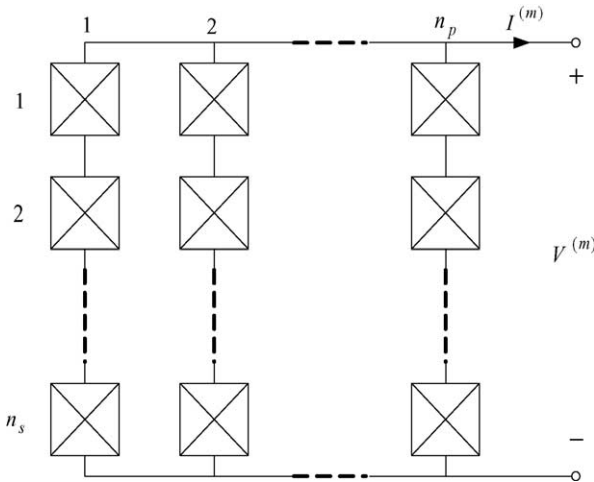$$I_{sc}^{(c)} = K_1 G_a \tag{24}$$

Fig. 13. The PV module arrangement.

$$K_2 = \frac{T_{\text{nom}}^{(c)} - T_{\text{a,nom}}}{G_{\text{a,nom}}} \quad (25)$$

$$T^{(c)} = T_a + K_2 G_a \quad (26)$$

$$V_{\text{oc}}^{(c)} = V_{\text{oc},0}^{(c)} - 2.3 \times \left(T^{(c)} - T_0^{(c)} \right) \quad (27)$$

$$V_t^{(c)} = \frac{1}{q} Ak \left(273 + T^{(c)} \right) \quad (28)$$

- *Step 3*. The final step is to determine the total PV module current for new operating conditions using Eq. (13), which can be rewritten as below in terms of individual cell parameters. Once steps 1–3 completed, it is possible to determine the output power of the PV module for that particular hour, using $P_{\max} = V_{\max} I_{\max}$:

$$I^{(m)} = n_p I_{\text{sc}}^{(c)} \left[1 - e^{[(V^{(m)} - n_s V_{\text{oc}}^{(c)}) + (n_s/n_p) R_s^{(c)} I^{(m)}]/n_s V_t^{(c)}} \right] \quad (29)$$

3.3. Modeling wind system

The wind speed can be considered as a random process assumed to be a Weibull distribution given by the following probability density function [14]:

$$f(v) = \frac{\beta v^{\beta-1}}{c^\beta} e^{-(v/c)^\beta} \quad (30)$$

where v is the wind speed in m/s, β the shape factor, and c the scale factor. Herein, the parameter β can be calculated approximately as $\beta = (\sigma/\bar{v})^{-1.086}$ and c can be given as below, which is a measure of characteristic speed associated with the average wind speed at the site. Where σ is the standard deviation, $\bar{v}$ the mean wind sped and Γ the complete gamma function:

$$c = \frac{\bar{v}}{\Gamma(1 + 1/\beta)} \quad (31)$$

Once the Weibull distribution functions are determined for wind speed over an every hour of a typical month, the average wind power output, P_{avg}^w for every hour of a typical day in each month can be easily calculated as follows:

$$P_{\text{avg}}^w = \int_0^\infty P^w f(v) \, dv \quad (32)$$

where P^w is the electric power output of the wind turbine at hour t is nonlinear with respect to wind speed v_t and can be expressed as below [15]:

$$P^w = \begin{cases} 0, & 0 \leq v_t < v_{\text{c-i}}, \\ P_N(a + bv_t + cv_t^2), & v_{\text{c-i}} \leq v_t < v_N, \\ P_N, & v_N \leq v_t < v_{\text{c-o}}, \\ 0, & v_t \geq v_{\text{c-o}} \end{cases} \quad (33)$$

where $v_{\text{c-i}}$, v_N and $v_{\text{c-o}}$ are the cut-in, nominal and cut-out wind speeds, respectively, for wind turbine generator. The
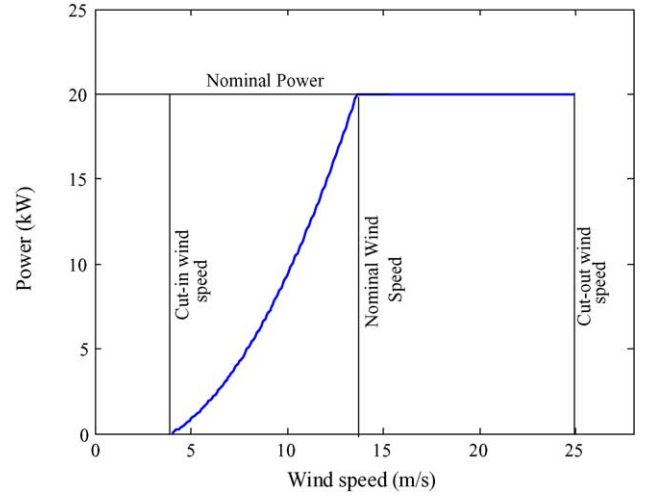

Fig. 14. Typical 20 kW wind unit output vs. wind speed.

constants, a, b and c are determined by the following equation:

$$a = \frac{1}{(v_{\text{c-i}} - v_N)^2} \left[v_{\text{c-i}}(v_{\text{c-i}} + v_N) - 4v_{\text{c-i}}v_N \left(\frac{v_{\text{c-i}} + v_N}{2v_N} \right)^3 \right],$$

$$b = \frac{1}{(v_{\text{c-i}} - v_N)^2} \left[4(v_{\text{c-i}} + v_N) \left(\frac{v_{\text{c-i}} + v_N}{2v_N} \right)^3 - (3v_{\text{c-i}} + v_N) \right],$$

$$c = \frac{1}{(v_{\text{c-i}} - v_N)^2} \left[2 - 4 \left(\frac{v_{\text{c-i}} + v_N}{2v_N} \right)^3 \right] \quad (34)$$

Eq. (33) can be linearized by taking the constants a and c as zero and $b = (v_t - v_{\text{c-i}})/(v_N - v_{\text{c-i}})$ for practical calculations. The plot of P^w for a 20 kW unit versus wind speed v is illustrated in Fig. 14.

It is clear from Fig. 14 that the power output increases nonlinearly between cut-in, $v_{\text{c-i}}$ and nominal wind speed, v_N, and stays at nominal power level within the wind speed variation of nominal, v_N and cut-out wind speed, $v_{\text{c-o}}$, at which the wind unit will be shut down for safety reasons.

3.4. Overall system evaluation

A MCS technique is used in this study, which reproduces the operation of the IMG system on an hourly basis. The hour by hour simulation processes takes into account the randomness of the load and renewable energy sources that is dependent upon the atmospheric conditions, namely wind and irradiance data. Failures of the generating units and times to repair are randomly generated according to mean failure rates and mean repair times. As well as these indices, other required reliability indices such as LOLE (loss of load expectation in h year^{-1}), LOEE (loss of energy expectation in MWh year^{-1}), FLOL (frequency of loss of load in occurrence year^{-1}) and LNSI (load not supplied per interruption in MW/occurrence) can be simulated by observing the system

capacity reserve model for a long time period [16]. Afterward, the simulation should be terminated when a stopping criterion is satisfied [17], which is given as below:

$$\frac{\sigma(X)}{NE(X)} \le \varepsilon_X \tag{35}$$

where X is the selected reliability index, ε_X the maximum error allowed and selected in this study as $\varepsilon_X = 0.05$. N the number of sampling years, both $E(X)$ and $\sigma(X)$ are the mean value and standard deviation of selected reliability index X, which are given as below:

$$E(X) = \frac{1}{N} \sum_{k=1}^{N} X_k \tag{36}$$

$$\sigma(X) = \sqrt{\frac{1}{N-1} \left[\sum_{k=1}^{N} (X_k^2 - NE^2(X)) \right]} \tag{37}$$

where X_k is the observed value of the index X in sampling year k.

The power available from all the generating units are combined based on the following assumptions. The main criteria that we considered herein are from the viewpoint of saving more fuel as well as maintaining system stability. Since the power delivered from the renewable energy sources fluctuates randomly based on wind and irradiance data, they cannot maintain power balance. WE output also depends on the load level due to operating constraints applied to maintain system stability. Hence, the assumptions made in this study are:

(1) Whereas a two state model (up state and down state) is used to model WE, DG and PV sources, three-state model, as explained in Section 3.1 (up state, derated state and down state) is used to model FC power plant.
(2) The PV system is operated at its full capacity when the system load level, L_i is greater than PV array capacity $P_{PV,i}$ in hour i.
(3) The remaining load is then shared jointly between wind and other system units, i.e. FC and DGs. This load dispatch is carried out based on the WE operating constraint, which is set to a specified fraction of the total load. This level is determined by a ratio of WE to FC plus DG energy, which is called dispatch ratio, r_D. As a result, the output of the WE is always adjusted to allow its maximum share in order to get maximum fuel saving.
(4) DG (diesel generators) and FC units are used to respond the load fluctuations through excitation/governor and inverter/hydrogen control in order to prevent the possible power imbalances between supply and demand.

The simulation process continues sequentially from 1 h to the next for repeated yearly samples until specified convergence criteria are satisfied. Once the number of system states of well-being model and their durations are recorded for entire system, the index of system loss of health expectation

(LOHE) and LOLE indices are computed as follows:

$$\text{LOHE} = [1 - P(h)] \times 8760 \tag{38}$$

$$\text{LOLE} = \frac{\sum_{i=1}^{n(r)} t(r)_i}{N} \tag{39}$$

where $P(h)$ is the probability of healthy state, which is given as Eq. (3).

Since the inputs of PV and WE units available naturally, their operating cost can be assumed to be almost zero with the exception of maintenance costs. Hence, the fuel energy savings (FES) due to the utilization of PV and WE units is almost equal to total energy delivered by them. If $P_{PV,i}$, $P_{WE,i}$, $P_{DG,i}$ and $P_{FC,i}$ are the photovoltaic, wind, diesel and fuel cell power outputs in hour i, the total FES by PV and WE can be calculated using Eq. (40) when the simulation is run for N sample years:

$$
\begin{aligned}
\sum \text{FES} &= (\text{FES})_{PV} + (\text{FES})_{WE} \\
&= \frac{1}{N} \left(\sum_{i=1}^{N \times \text{yearly hours}} P_{PV,i} \right) \\
&\quad + \frac{1}{N} \left(\sum_{i=1}^{N \times \text{yearly hours}} P_{WL,i} \right) \\
&= \frac{1}{N} \left[\sum_{i=1}^{N \times \text{yearly hour}} (P_{PV,i} + P_{WL,i}) \right]
\end{aligned} \tag{40}
$$

where

$$P_{WL,i}$$

$$= \begin{cases} (P_{DG,i} + P_{FC,i})r_D & \text{for } P_{WE,i} > (P_{DG,i} + P_{FC,i})r_D, \\ L_i & \text{for } P_{WE,i} < (P_{DG,i} + P_{FC,i})r_D \end{cases}$$

FC output voltage, accordingly its power goes down progressively as the electrodes and electrolyte getting older. This situation can be characterized as decline of voltage in units of mV h^{-1} or percent power deterioration/h. Hence, a degradation rate of ε_d kW/1000 h can be incorporated to the FC energy conversion model as below for steady-state nominal output power, where in this study, a degradation rate is considered as $\varepsilon_d = 0.5$, and t is the operation time on the basis of 1000 h:

$$P_{FC} = P_{FC,\text{nom}} - \varepsilon_d t \tag{41}$$

4. Case studies

The proposed evaluation model has been applied to a sample IMG system. The generating units in the example system and their reliability data are given in Table 2. The rated power of a 918 W_{peak} PV array, consisting of nine groups of

Table 2
Generating units of IMG system and their reliability data

Generating units	Nominal power (kW)	Failure rate (failures year^{-1})	Repair time (h)	Forced outage rate (FOR)
Base system				
DG unit-II	50	9.42	50	0.0510
FC init	50–0.5t	4.32	40	0.0197
A total capacity of 40 kW added to base system in six cases				
Case I				
1 DG unit	40	9.25	45	0.0453
Case II				
1 FC unit	40–0.5t	4.28	40	0.0195
Case III				
1 DG unit	20	8.24	30	0.0274
1 FC unit	20–0.5t	4.26	35	0.0170
Case IV				
44 PV arrays	40.392	4.56	80	0.0399
Case V				
2 WE units	40	4.56	80	0.0399
Case VI				
22 PV arrays	20.196	4.52	75	0.0372
1 WE unit	20	4.56	80	0.0399

Fig. 15. System health for the cases in Table 2.

three series modules with 34 W$_{peak}$, and a 20 kW wind energy unit (cut-in, nominal and cut-out speeds are 4, 13.62 and 24.92 m s^{-1}, respectively) as well as 40 kW FC unit are considered in six cases for adding a total capacity of 40 kW power unit, which are summarized in Table 2. Since FC output power has a continuous degradation rate and has a reliability model that is subject to a number of possible outage and derated states due to partial or full failure of auxiliaries, the reliability data such as nominal power, MTTF (MTTF = 1/failure rate) and repair time are updated every year according to the proposed FC model.

The IEEE-RTS load profile with a peak of 70 kW given in Table 3 [18] is used together with Table 2 data in order to simulate the hourly operation of the IMG system. The weekly, daily and hourly peak load values are given in percent of annual, weekly and daily peak loads, respectively, so that one can maintain the same load shape for different annual peaks.

Fig. 15 compares the system degree of health in meeting the deterministic loss of the largest/large unit for the six cases
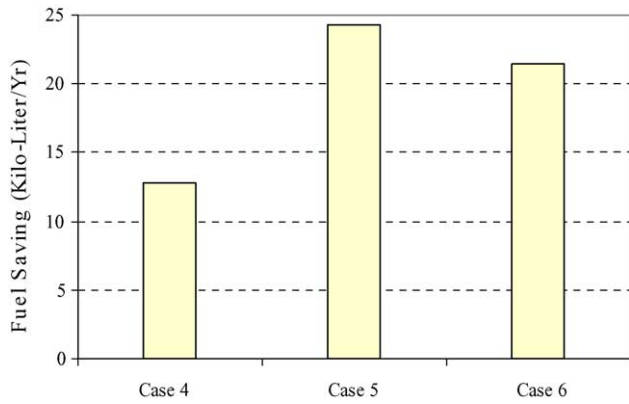
Table 3
Load profile for the IMG system

	1[a]	2	3	4	5	6	7	8	9	10	11	12	13	14	15	16	17	18	19	20	21	22	23	24	25	26
Weakly loads in percent of annual peak																										
Peak load	86	90	87	83	88	84	83	81	74	73	71	73	70	75	72	80	75	84	87	88	86	81	90	89	90	86
Week	27	28	29	30	31	32	33	34	35	36	37	38	39	40	41	42	43	44	45	46	47	48	49	50	51	52
Peak load	76	82	80	88	72	78	80	73	73	71	78	70	72	72	74	74	80	88	89	90	94	89	94	97	100	95

	Monday		Tuesday		Wednesday		Thursday		Friday		Saturday		Sunday
Daily peak load in percent of weekly peak													
Peak load	93		100		98		96		94		77		75

	1[b]	2	3	4	5	6	7	8	9	10	11	12	13	14	15	16	17	18	19	20	21	22	23	24
Hourly peak load in percent of daily peak																								
Winter weeks																								
Weekday	67	63	60	59	59	60	74	86	95	96	96	95	95	95	93	94	99	100	100	96	91	83	73	63
Weekend	78	72	68	66	64	65	66	70	80	88	90	91	90	88	87	87	91	100	99	97	94	92	87	81
Summer weeks																								
Weekday	64	60	58	56	56	58	64	76	87	95	99	100	99	100	100	97	96	96	93	92	92	93	87	72
Weekend	74	70	66	65	64	62	62	66	81	86	91	93	93	92	91	91	92	94	95	95	100	93	88	80
Spring/fall weeks																								
Weekday	63	62	60	58	59	65	72	85	95	99	100	99	93	92	90	88	90	92	96	98	96	90	80	70
Weekend	75	73	69	66	65	65	68	74	83	89	92	94	91	90	90	86	85	88	92	100	97	95	90	85

[a] Weeks.
[b] Hours.

Fig. 16. Fuel savings for the cases of renewable energy additions as in Table 2.

Fig. 18. Excess renewable energy vs. load growth for three cases of renewable energy additions.

with the base system in Table 2. It is evident from Fig. 15 that system health increases for each capacity addition but with different degrees. Fig. 15 shows that the reliability of DG and FC units are better than that of renewable energy sources. However, a significant cost–benefit can be obtained by utilizing PV or WE units because of the fuel savings. Fig. 16 compares the fuel savings for the cases with renewable energy sources adding. Fuel savings herein are calculated by taking a heat rate of $3.2\,kWh\,l^{-1}$.

System reliability degree falls with the increase in peak load if the power sources are maintained at the same level. Fig. 17 compares the decrease in reliability with increase in peak load for the six cases of 40 kW capacity additions. It can be observed that conventional and FC units as well as a mix of these units reflect very similar reliability level. The reliability benefits from DG and FC unit additions are relatively higher at higher loads.

The energy available from the output of renewable energy sources may not always be consumed due to system constraints or short period lower demands. Fig. 18 compares the total excess energy wasted per year versus load growth. It can be observed that most of the generated power from renewable sources is consumed except for the lower peak loads in the case of adding only WE source.
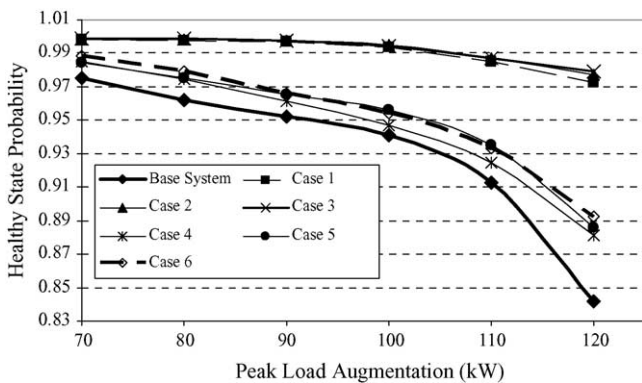
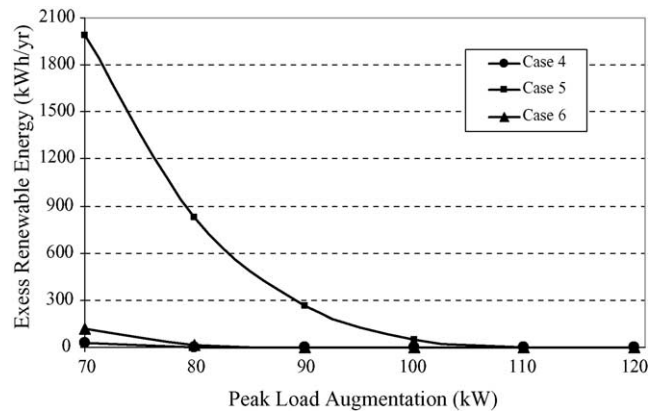Because change in the shape of load curve has an effect on the system reliability and cost indices, the augmentation in the system load in above simulations is generated from the load profile given in Table 3 so as to maintain the same load shape. Since the output out of renewable energy sources are based on the atmospheric conditions, maximum benefit in utilizing WE and PV sources can be achieved at an appropriate rate of combination of these sources and this rate may vary dependent upon the location of the site.

Significant benefits can be achievable by capacity expansion of PV and WE energy in IMG systems. However, renewable energy capacity adding may provide maximum benefit at certain capacity adding levels. Fig. 19 compares the increase in renewable energy adding to IMG system for the cases of 70 and 100 kW peak loads. It is evident from Fig. 19 that the curves saturate in all cases after a certain level of renewable energy adding. It can be suggested from this study that although we have significant savings in operating cost, desired reliability level versus load growth may not be achievable by adding only renewable energy.

The above simulations assume that all available energy from WE output can be consumed to meet the system load requirements. However, benefits from WE penetration,

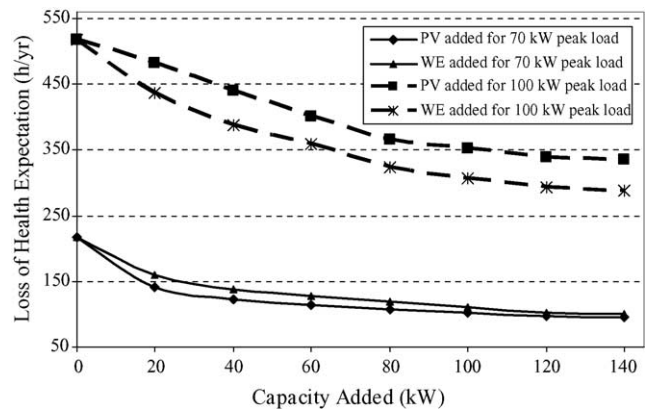Fig. 17. System health vs. load growth.

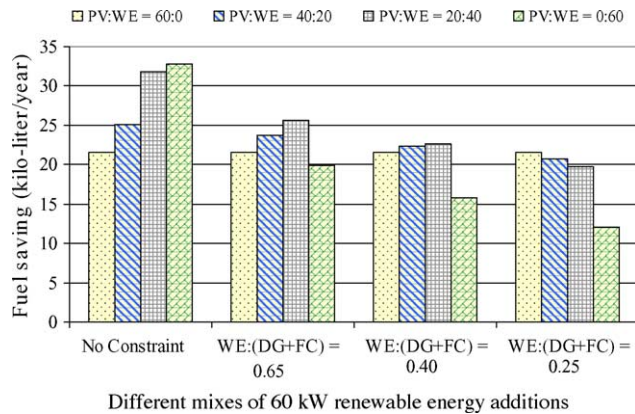Fig. 19. The effect of PV and WE capacity adding on LOHE.

Fig. 20. Effect of WE constraints on system operating cost.

particularly in independent systems, are limited due to operating constraints applied to maintain system stability. In order to consider the effect of this dispatch ratio on fuel savings, system is modified by replacing 40 kW capacity additions with 60 kW for the cases of renewable energy injections. The capacity of 60 kW is added to the base system as the following mixes of PV:WE: 60:0, 40:20, 20:40, 0:60. Fig. 20 compares these four mixes of PV and WE for the following four different operation modes of: no WE constraint, a WE to FC plus DG dispatch ratio of 0.65, 0.40 and 0.20, respectively. The constraint of dispatch ratio, $r_D = WE/(FC + DG) = 0.65$, 0.40 and 0.25 indicates that the output of WE cannot exceed 39, 28 and 20% of the total system load, respectively. It is evident from Fig. 20 that as the constraint of dispatch ratio, r_D decreases, the cost–benefits from higher WE penetration reduces more.

The cost–benefits of IMG system including FC, PV and WE can also be expanded on different hybrid configuration of these sources in order to make better use of their operating characteristics. For instance, the FC power plan used in this study consists of a fuel-processing unit (reformer), FC stack and power conditioning unit. By replacing reformer with electrolyzer subsystem, the FC could be combined with the PV and WE. Hence hybrid fuel cell system with WE and PV could be more efficient than that obtained from individual utilizations in an IMG system. In this case, for example, if the renewable energy sources have excess energy, then this energy can be sent to the electrolyzer to recharge the hydrogen storage. Thus, the waste energy because of the dispatch ratio and low load demand can be converted to savings.

5. Conclusions

In this paper, a reliability and cost evaluation of alternate energy utilization in an independent micro-grid community is presented. The paper presents the models of fuel cell power plant, wind energy and photovoltaic system. The paper offers practical conceptions concerning the types of energy sources and their penetration levels in order to satisfy the load requirements and load growth for the IMG system.

One of the essential conclusions that can be drawn in this study is that the determination of cost effective capacity expansion and the corresponding investment plan requires a comparative study of a number of alternative schemes. Operating constraints and geographic locations are also the factors that can affect the capacity planning decisions. The figures presented in this paper should assist the power system engineers to decide on the types and mixes of various energy sources, the cost effective operating policies, and an appropriate expansion plan to satisfy the demand augmentation in an IMG system.

Acknowledgements

References

[1] Newfoundland & Labrador Hydro, Isolated systems generating planning practices: a survey of Canadian utilities, November 1995.

[2] R. Billinton, F.-F. Mahmud, A. Saleh, An approach to evaluating system well-being in engineering reliability applications, Reliab. Eng. Syst. Safety 50 (1) (1995) 1–5.

[3] L. Goel, L.S. Low, Composite power system adequacy assessment in terms of well-being, Comput. Electr. Eng. 28 (6) (2002) 501–512.

[4] R. Billinton, R. Karki, Application of Monte Carlo simulation to generating system well-being analysis, IEEE Trans. Power Syst. 14 (3) (1999) 1172–1177.

[5] Y.G. Hegazy, M.M.A. Salama, A.Y. Chikhani, Adequacy assessment of distributed generation systems using Monte Carlo simulation, IEEE Trans. Power Syst. 18 (1) (2003) 48–52.

[6] R. Karki, R. Billinton, Reliability/cost implications of PV and wind energy utilization in small isolated power systems, IEEE Trans. Energy Conv. 16 (4) (2001) 368–373.

[7] D. Thirumalai, R.E. White, Mathematical modelling of proton-exchange-membrane fuel-cell stacks, J. Electrochem. Soc. 144 (1997) 1717–1723.

[8] C.E. Thomas, Direct-hydrogen-fueled proton-exchange-membrane fuel cell system for transportation applications, Ford Motor Company and U.S. Department of Energy Office of Transportation Technologies, May 1997.

[9] J.M. Cunningham, A.H. Myron, J.F. David, A comparison of high-pressure and low-pressure operation of PEM fuel cell systems, in: Proceedings of the SAE International, 2001, p. 538.

[10] S. Pischinger, C. Schönfelder, W. Bornscheuer, A.W. Kindl, Integrated air supply and humidification concepts for fuel cell systems, in: Proceedings of the SAE International, 2001, p. 233.

[11] M. Tanrioven, M.S. Alam, Reliability modeling and assessment of grid-connected PEM fuel cell power plants, J. Power Sources 142 (1–2) (2005) 264–278.

[12] A. Joyce, C. Rodrigues, R. Manso, Modelling a PV system, Renewable Energy 22 (1–3) (2001) 275–280.

[13] J.A. Gow, C.D. Manning, Development of a photovoltaic array model for use in power electronics simulation studies, IEE Proc. Electric Power Appl. 146 (2) (1999) 193–200.

[14] S.H. Karaki, R.B. Chedid, R. Ramadan, Probabilistic production costing of diesel-wind energy conversion systems, IEEE Trans. Energy Conv. 15 (3) (2000) 284–289.

[15] R. Billinton, B. Guang, Adequacy evaluation of generation systems including wind energy, in: Proceedings of the IEEE Canadian Conference on Electrical and Computer Engineering, vol. 1, CCECE 2002, 12–15 May, 2002, pp. 24–29.

[16] R. Billinton, R.N. Allan, Reliability Evaluation of Power Systems, 2nd ed., Plenum Publishing, New York, 1996.

[17] R. Billinton, C. Hua, R. Ghajar, A sequential simulation technique for adequacy evaluation of generating systems including wind energy, IEEE Trans. Energy Conv. 11 (4) (1996) 728–734.

[18] Reliability Test System Task Force of the Application of Probability Methods Subcommittee, IEEE Reliability Test System, IEEE Trans. Power Apparatus Syst. PAS-98 (6) (1979) 2047–2054.